Computational study of Ca, Sr and Ba under pressure

2006 J. Phys.: Condens. Matter 18 4623

(http://iopscience.iop.org/0953-8984/18/19/016)

INSTITUTE OF PHYSICS PUBLISHING JOURNAL OF PHYSICS: CONDENSED MATTER

J. Phys.: Condens. Matter **18** (2006) 4623–4640 doi:10.1088/0953-8984/18/19/016

Computational study of Ca, Sr and Ba under pressure

F Jona and P M Marcus

Department of Materials Science and Engineering, State University of New York, Stony Brook, NY 11794-2275, USA

Received 7 November 2005, in final form 3 April 2006
Published 26 April 2006
Online at stacks.iop.org/JPhysCM/18/4623

Abstract

A first-principles procedure for the calculation of equilibrium properties of crystals under hydrostatic pressure is applied to Ca, Sr and Ba. The procedure is based on minimizing the Gibbs free energy G (at zero temperature) with respect to the structure at a given pressure p, and hence does not require the equation of state to fix the pressure. The calculated lattice constants of Ca, Sr and Ba are shown to be generally closer to measured values than previous calculations using other procedures. In particular for Ba, where careful and extensive pressure data are available, the calculated lattice parameters fit measurements to about 1% in three different phases, both cubic and hexagonal. Rigid-lattice transition pressures between phases which come directly from the crossing of $G(p)$ curves are not close to measured transition pressures. One reason is the need to include zero-point energy (ZPE) of vibration in G. The ZPE of cubic phases is calculated with a generalized Debye approximation and applied to Ca and Sr, where it produces significant shifts in transition pressures. An extensive tabulation is given of structural parameters and elastic constants from the literature, including both theoretical and experimental results.

1. Introduction

We report here the results of a comprehensive computational first-principles study of the crystal structures of the heavy alkaline-earth metals, and the changes of those structures in response to increasing hydrostatic pressure. These elements (Ca, Sr, Ba) are electronically fairly simple (s–p bonded) at ambient pressure: below the Fermi level E_F the electronic bands are practically free-electron-like, while the broad and almost unoccupied d bands are slightly above E_F. As a consequence, near E_F the electronic wavefunctions are modified by hybridization with the d bands: increasing hydrostatic pressure increases the amount of d occupation, changing the bonding and thereby inducing phase transitions. Ca and Sr are face-centred cubic (fcc) at ambient pressure, but become body-centred cubic (bcc) at pressures in the low kilobar range, with further transitions at higher pressures; Ba, for which the d occupation is greater than for Ca and Sr, is already bcc at ambient pressure, but becomes hexagonal close packed (hcp) with increasing pressure, exhibiting then other transitions at higher pressures.

The pressure-induced phase transitions in Ca, Sr and Ba were established by several experiments in the course of the past forty years. Early work was done with piston-based or tungsten-anvil instrumentation, more recent work with diamond-anvil cells either without or with pressure-transmitting fluids such as silicone and mineral oil. Some of the higher-pressure phases originally reported were later found to be incorrect, and some are still unidentified, to date. Experiments with energy-dispersive x-ray diffraction and neutron inelastic scattering also produced values of the lattice parameters and elastic constants, sometimes with surprisingly large disagreements among different workers, particularly for the elastic constants. Pertinent details will be discussed below.

Previous theoretical studies were aimed at the identification of ground states, the determination of transition pressures and the calculations of structural parameters; elastic constants were calculated at zero pressure. The techniques used for these purposes were mostly based on pseudopotential methods or linear muffin-tin orbital (LMTO) procedures or augmented plane-wave schemes. Agreement with experimental results was not always good, particularly with regard to elastic constants, as discussed below for each of the three elements considered.

The work reported in this paper was directed toward calculations of lattice parameters of both ground states and high-pressure phases, together with transition pressures and elastic constants, mainly at zero pressure; we used procedures different from previous studies. We have also introduced the effects of zero-point energy (ZPE) on the transition pressures of Ca and Sr. The ZPE is calculated in the generalized Debye approximation, and hence gives only an approximate idea of the effect on transition pressures. In the case of Sr, but not of Ca, the effect of the pressure dependence of the ZPE on the transition pressure is estimated and found to be small. Hence, for Ca the approximation is made that the difference in ZPE of the two phases of the transition is independent of pressure. The calculation procedures are briefly described in section 2. Results and comparisons with literature data are given for Ca in section 3, for Sr in section 4 and for Ba in section 5. A discussion of the results is presented in section 6.

2. Calculation procedures

The energies of structures were calculated with the WIEN2k computer program developed by Blaha and co-workers [1]. This program uses the FPLAPW (full-potential linearized augmented plane-wave) method for computation of the electronic structure of solids from the Kohn–Sham equations of density functional theory [2, 3] in the generalized gradient approximation (GGA). Two procedures were employed to find the minima of the free energy $G = E + pV$ (at $T = 0$ K) (E = energy per atom, V = volume per atom) as a function of the tetragonal or hexagonal lattice parameters a and c. One procedure used the MNP (minimum-path) program, which makes hops toward the minimum of G in strain space (two-dimensional for tetragonal and hexagonal structures) based on the local gradient and local curvature of the free energy at a given structure. Convergence is usually achieved in five or six hops [4]. A second procedure consists in tracing out G continuously on the epitaxial Bain path (EBP) until a minimum is reached, which is then a minimum of G for all variations of a and c around equilibrium. The EBP at any pressure p and a given a is defined by a boundary condition on the energy E as a function of c that contains p [5]. Usually the MNP was applied first with a small number of k-points to give an approximate structure, which was then refined by following the EBP with more accurate G values.

The parameters used in the WIEN program for Ca and Sr were: muffin-tin radius RMT = 2.0 bohr; plane-wave cut-off $RK_{max} = 8.0$; largest vector in the charge-density Fourier expansion GMAX = 16 bohr^{-1}; k-point sampling in the Brillouin zone of 16 000 points (1183

Table 1. Experimental transition pressures in Ca, Sr and Ba. The abbreviations for the structures are: fcc = face-centred cubic; bcc = body-centred cubic; sc = simple cubic; hcp = hexagonal close packed. The numbers above the arrows are the experimental transition pressures in kbar. For Ca and Sr most of the experimental results are due to Olijnyk and Holzapfel (OH) [6], for Ba, to Takemura (T) [22], with other workers' modifications as indicated. It is important to note that the OH experiments were done with no pressure-transmitting medium, and hence the nominal pressure cited 'may overestimate the hydrostatic pressure component by 10 to 40 kbar' [6].

Exp. ref.	Transitions
	Ca
OH [6]	fcc (Ca I) $\xrightarrow{195}$ bcc (Ca II) $\xrightarrow{320}$ sc (Ca III) $\xrightarrow{420}$? (Ca IV) $\left(\xrightarrow{1120}\right.$ hcp (Ca V)[(a)]$\left.\right)$
	Sr
OH [6]	fcc (Sr I) $\xrightarrow{35}$ bcc (Sr II) $\xrightarrow{260}$ 'β-tin' (Sr III)[(b)] $\xrightarrow{350}$? (Sr IV) $\xrightarrow{460}$ incommens. (Sr V)[(c)]
	Ba
T[(d)] [22]	bcc (Ba I) $\xrightarrow{55}$ hcp (Ba II) $\xrightarrow{126}$ incommens. (Ba IV)[(e)] $\xrightarrow{450}$ hcp (Ba V)

[(a)] The transition to hcp was suggested by theoretical studies of Ahuja *et al* [12], but not confirmed experimentally.
[(b)] Sr III was originally believed to be 'related to the structure of Ca III by an orthorhombic distortion' [6] and later claimed to be orthorhombic [15], but finally proven to be tetragonal with the β-tin structure by McMahon *et al* [16].
[(c)] Sr V was shown by McMahon *et al* [16] to have the same incommensurate structure composed of a 'host' and two or more 'guest' components as Ba IV.
[(d)] The early studies reported a transition to a nonidentified structure Ba III at about 75 kbar (see the references cited in [22]), but Takemura found no evidence of this phase III and speculated that this phase 'may exist only at high temperature and high pressure' [22].
[(e)] The structure of Ba IV was found by Nelmes *et al* [25] to be composed of a tetragonal 'host' with 'guest' chains incommensurate with the host in channels along the *c* axis of the host (see also the comment by Heine [26]).

in the irreducible wedge IBZ); criterion for energy convergence 1×10^{-6} Ryd. For Ba the only changes were: RMT = 2.4 bohr, number of k-points 32 000 (2176 in the IBZ) for the bcc structure and 16 000 (900 in the IBZ) for the hcp structure.

3. Calcium

3.1. Review

Calcium has the face-centred-cubic (fcc) structure at ambient pressure, but exhibits phase changes when the pressure is increased. These pressure-induced phase transitions were established by a number of experiments since 1963 (references to earlier and recent papers are given in the following tables). Transition pressures were established most reliably by an experiment with energy-dispersive x-ray diffraction at room temperature and pressures up to 460 kbar done by Olijnyk and Holzapfel (OH) in 1984 [6]. Although now more than 20 years old, this work is still the most complete experimental investigation of the alkaline earths under pressure. But with regard to transition pressures it is important to keep in mind that the experiment was done 'without any additional pressure-transmitting fluid' and that therefore the pressure values quoted 'may overestimate the hydrostatic pressure component by (10–40 kbar) due to nonhydrostatic stresses especially in the upper pressure range' [6]. The finding of interest to the present study is that Ca transforms from fcc at zero pressure (Ca I) to bcc (Ca II) at 195 kbar (for $V/V_0 = 0.59$ and volume change $\Delta V \sim 2\%$), then to simple cubic (sc) (Ca III) at 320 kbar and finally to an unidentified phase (Ca IV) at 420 kbar. For convenience, these results are summarized concisely in table 1, top panel. Unfortunately, OH's paper does not

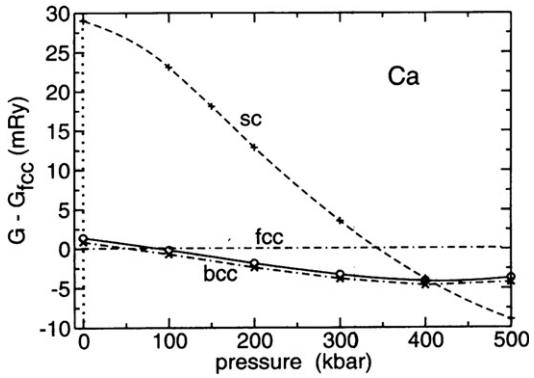

Figure 1. Free-energy differences for Ca bcc–fcc (circles and crosses) and sc–fcc (plus signs) versus pressure. The circles exclude, the crosses include, zero-point energies.

give explicit values of the lattice constants and their pressure dependence, but a table lists d-spacings[1] and intensity ratios for Ca II (bcc) at 265 kbar and for Ca III (sc) at 390 kbar.

Theoretically, the earliest most complete study of the pressure-induced fcc-to-bcc phase transitions in the heavy alkaline earths was done by Animalu in 1967 [7], who did the analysis in terms of Gibbs free energies and also estimated the contributions of the zero-point energies for Ca, Sr and Ba. However, Animalu's work found the wrong ground state for Ca at ambient pressure, obtaining lower energy for the bcc rather than the observed fcc phase. Later pseudopotential calculations by Moriarty [8] found the correct ground state for Ca and Sr, but not for Ba. The correct sequence of structures for increasing pressure was found by Skriver [9] for all three elements using the LMTO-ASA method. For Ca the fcc-to-bcc transition was modelled by Wentzcovitch and Krakauer [10] and analysed by Sliwko *et al* [11] with FPLAPW-LDA calculations, while the bcc-to-sc transition was investigated by Ahuja *et al* [12]. These authors also predicted that a transition from sc to hcp would occur at about 1120 kbar. The results of these and other studies will be discussed and compared to ours in the next section.

3.2. Results and discussion

At zero pressure we find the bcc phase to have a G value about 1.4 mRyd/atom, and the sc phase about 29 mRyd/atom, higher than the fcc phase, thus establishing the fcc phase as the ground state, in accordance with experiment. Experimental and theoretical values of the lattice parameters are given in the upper panel of table 2. Our results for lattice parameters at $p = 0$ agree with the available experimental data to within less than 1%, mostly better than theoretical values published in the literature. At higher pressures, data on lattice parameters are very scarce. As mentioned above, we could only find the experimental values of the crystallographic d-spacing as given by Olijnyk and Holzapfel [6] at one pressure for the bcc phase and another pressure for the sc phase. From the d-spacings we calculated the value of a listed in the table. Our interpolated results, also listed in the table, agree with the experimental data within 0.4 and 1.3%, respectively.

The Gibbs free energy G was calculated as a function of pressure for all three cubic structures exhibited by Ca: the fcc, the bcc and the sc structure. Figure 1 depicts the differences $G_{\rm bcc} - G_{\rm fcc}$ and $G_{\rm sc} - G_{\rm fcc}$ as functions of pressure. If we define the rigid-lattice

[1] 'd-spacings' is the term used to indicate the distances between identical planes of atoms in a crystal according to Bragg's law $2d \sin\theta = n\lambda$. For cubic crystals the distance between $\{hk\ell\}$ planes is $d_{hk\ell} = a/\sqrt{h^2 + k^2 + \ell^2}$.

Table 2. Lattice parameters of Ca, Sr and Ba. The abbreviations for the structures are: fcc = face-centred cubic; bcc = body-centred cubic; sc = simple cubic; hcp = hexagonal close packed. p is the pressure in kbar; a and c for fcc structures are the lattice parameters of the body-centred tetragonal cell in Å (if a_0 is the parameter of the conventional fcc cell, then $a = a_0/\sqrt{2}$ and $c = a_0$). The a values in parentheses were calculated from $c = a_0$ as given. The experimental data are room temperature values unless indicated otherwise. (int.) = interpolated values; (from d) = calculated from tables of experimental d spacings; (from V) = calculated from the values of the reported equilibrium volume.

Exp./Theo. + [Ref.]	p	Structure	a	c	c/a
		Ca			
Exp. Donohue [30]	0	fcc	(3.951)	5.588	$\sqrt{2}$
Exp. Pearson [31]	0	fcc	(3.9516)	5.5884	$\sqrt{2}$
Theo. this work	0	fcc	3.925	5.532	1.409
Exp. cited by Moriarty (from V) [8]	0	fcc		5.56	
Theo. Sliwko *et al* (from V) [11]	0	fcc		5.34	
Theo. Wentzcovich + Krakauer [10]	0	fcc		5.50	
Theo. Mehl + Papaconstantopoulos [17]	0	fcc		5.30	
Exp. Olijnyk + Holzapfel (from d) [6]	265	bcc	3.559		
Theo. this work (int.)	265	bcc	3.574		
Exp. Olijnyk + Holzapfel (from d) [6]	390	sc	2.614		
Theo. this work (int.)	390	sc	2.649		
		Sr			
Exp. Donohue [30]	0	fcc	(4.303)	6.086	$\sqrt{2}$
Exp. Pearson [31]	0	fcc	(4.296)	6.076	$\sqrt{2}$
Theo. this work	0	fcc	4.280	6.052	1.414
Exp. cited by Moriarty (from V) [8]	0	fcc		6.05	
Theo. Sliwko *et al* (from V) [11]	0	fcc		5.77	
Theo. Mehl + Papaconstantopoulos [17]	0	fcc		5.73	
Exp. McWahn + Jayaraman [19]	42	bcc	4.434		
Theo. this work (int.)	42	bcc	4.378		
		Ba			
Exp. Pearson [31]	0	bcc	5.013		
Exp. Donohue [30]	0	bcc	5.023		
Exp. Pearson $T = 5$ K [31]	0	bcc	5.000		
Theo. this work	0	bcc	5.034		
Theo. Mehl + Papaconstantopoulos [17]	0	bcc	4.82		
Theo. Chen *et al* [32]	0	bcc	4.80		
Exp. Takemura (int.) [22]	60	hcp	3.909	6.147	1.57
Theo. this work (int.)	60	hcp	3.930	6.075	1.55
Theo. Chen *et al* [32]	0	hcp	4.30	6.73	1.56

transition pressure between two phases as the pressure at which the corresponding G-functions cross, i.e., at which the G-difference vanishes, we find that the fcc-to-bcc transition occurs at about 90 kbar, and the bcc-to-sc transition at 400 kbar, compared with 195 and 320 kbar, respectively, as found experimentally by Olijnyk and Holzapfel [6]. The discrepancy between these results may be explained partially by the uncertainty in the experimental results due to nonhydrostaticity (mentioned above and in the caption to table 1), and partially by the effect of different zero-point energies (ZPE) in the phases involved.

To investigate the extent to which ZPE can affect transition pressures we have developed a procedure based on the generalized Debye approximation (elastic wave velocities are functions

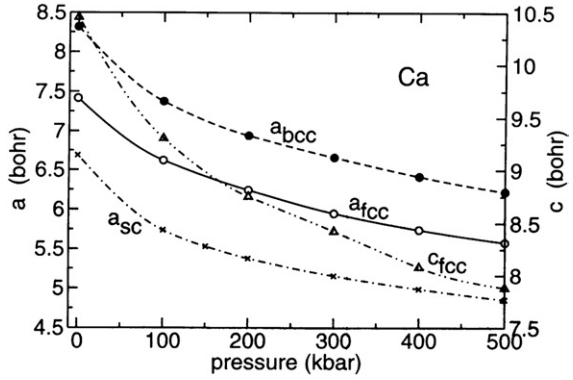

Figure 2. Pressure dependence of the lattice parameters of fcc, bcc and sc Ca.

of direction). Because of this approximation the result of this procedure is to be considered only an approximate ZPE correction of the equilibrium free energy of the rigid lattice. An efficient accurate procedure for calculating the Debye theta for cubic structures is described in the appendix; the procedure requires knowledge of the lattice parameters, the elastic constants and the density of a phase.

Table 3, upper panel, lists the available experimental results for the elastic constants of Ca at zero pressure, together with some theoretical results published in the literature, and our own. It is surprising to find large discrepancies between different experimental results (from 36% for c_{44} to 74% for c_{11}), and similar discrepancies between different theoretical results (some of these even find the fcc phase unstable, since C' is negative). Our results were obtained with the procedure described elsewhere using the second strain derivatives of G [13]. For fcc Ca the agreement with experiment cannot be evaluated with confidence, owing to the large experimental uncertainty, but is at best about 8% for c_{11} and about 20% for c_{44}; for bcc Ca no experimental results are available, since the phase does not exist at zero pressure.

With our values of the lattice constants (table 2) and of the elastic constants (table 3), we find within the Debye approximation a ZPE of 1.42 and 0.88 mRyd/atom for fcc and bcc Ca, respectively. Comparisons with literature values are somewhat questionable, since we were able to find only two rather old values (38 and 32 years old, respectively) for the ZPE of fcc and bcc Ca: 2.03 and 1.98 mRyd/atom, respectively, given by Animalu [7], and 1.69 and 1.62 mRyd/atom, respectively, by Moriarty [8]. Correcting our zero-pressure values of the free energies with our ZPE results we find that the fcc phase is now only 0.86 mRyd lower in energy than the bcc phase, but still the ground state. Since the ZPE is expected to increase with pressure it should be calculated again at finite pressures, which in turn requires calculations of the elastic constants of all phases at finite pressures. We have not made those calculations for Ca at this time (see section 4.2), but adopted the simple approximate assumption that the difference in ZPE would remain constant with increasing pressure, and corrected the free-energy values accordingly. Figure 1 includes the corrected G-difference curves, whence we see that the fcc-to-bcc transition moves from 90 to about 56 kbar, and the bcc-to-sc transition from 400 to about 412 kbar, actually increasing the disagreement with the experimental result of Olijnyk and Holzapfel [6]. Comparisons between experimental and theoretical results from the literature are given in the annotated table 4.

Useful by-products of the calculations of the free energies at finite pressures are the pressure dependences of the lattice constants and the volumes. Figure 2 depicts the lattice

Table 3. Elastic constants of Ca, Sr and Ba. The abbreviations for the structures are: fcc = face-centred cubic; bcc = body-centred cubic; $C' = (c_{11} - c_{12})/2$; $B = (c_{11} + 2c_{12})/3$; $\mu = (2C' + 3c_{44})/5$. The numbers in parentheses were calculated from the data reported explicitly in the papers cited. All elastic constants in Mbar. The experimental results apply to room temperature (unless otherwise indicated), the theoretical results, to 0 K and $p = 0$.

Exp./Theo. + [Ref.]	Structure	c_{11}	c_{12}	c_{44}	C'	B	μ
			Ca				
Exp. Smithells Handbook [20]	fcc	0.16	0.08	0.12	(0.04)	(0.107)	
Exp. Stassis *et al* [33]	fcc	0.278 01	0.182 25	0.163 04	(0.04788)	(0.21417)	
Exp. Heiroth *et al* [34]	fcc	0.228	(0.160)	0.14	0.034	(0.013)	
Theo. this work	fcc	0.209	0.136	0.111	(0.0365)	(0.160)	
Theo. Mehl + Papaconstantopoulos [17]	fcc	0.15	0.10	0.04	(0.025)	(0.117) 0.21[a]	
Theo. Wang *et al* [35]	fcc	0.227	0.144	0.210	(0.0415)	0.172	
Theo. Pollack *et al* [18]	fcc				−0.015	0.17	0.075
Theo. Sliwko *et al* [11]	fcc	0.231	0.172		0.029	0.192	
Theo. Pollack *et al* [18]	bcc				−0.002	0.159	0.092
Theo. Sliwko *et al* [11]	bcc	0.237	0.183		0.027	0.201	
Theo. this work	bcc	0.145	0.141	0.159	(0.02)	(0.142)	
			Sr				
Exp. Buchenau *et al* [36]	fcc	0.17 ± 8	(0.120)	0.099	0.0248		
Exp. Smithells Handbook [20]	fcc	0.147	0.099	0.0574	(0.0975)	(0.115)	
Theo. this work	fcc	0.137	0.096	0.0598	(0.0205)	(0.110)	
Theo. Mehl + Papaconstantopoulos [17]	fcc	0.08	0.03	−0.03	(0.055)	(0.047) 0.15[a]	
Theo. Pollack *et al* [18]	fcc				−0.011	0.125	0.054
Theo. Sliwko *et al* [11]	fcc	0.189	0.153		0.018	(0.165)	
Exp. Mizuki + Stassis $T = 930$ K [21]	bcc	0.109 35	0.076 94	0.074 08	(0.01620)	(0.08774)	
Theo. this work (int.)	bcc	0.140	0.098	0.156	(0.021)	(0.112)	
Theo. Sliwko *et al* [11]	bcc	0.206	0.136		0.035	(0.159)	
Theo. Pollack *et al* [18]	bcc				−0.001	0.117	0.067
			Ba				
Exp. Mizuki + Stassis [21]	bcc	0.081 18	(−0.00376)	0.101 08	0.042 47		
Exp. Buchenau *et al* [36]	bcc	0.10 ± 0.03	(0.0542)	0.095 ± 0.005	0.0229 ± 0.001		
Theo. this work	bcc	0.122	0.045	0.106	(0.0385)	(0.0707)	
Theo. Mehl + Papaconstantopoulos [17]	bcc	0.09	0.07	0.13	(0.01)	(0.077) 0.10[a]	
Theo. Öztekin *et al* [37]	bcc	0.129	0.061	0.066			
Theo. Pollack *et al* [18]	bcc				−0.001	0.104	0.055

[a]The value in parentheses was calculated from c_{11} and c_{12} as given in table III of [17], contradicting the value of B given in table I of the same paper.

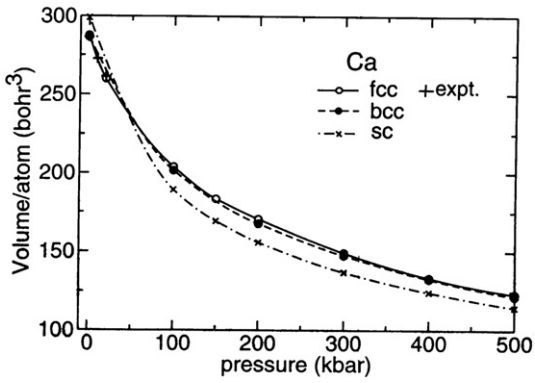

Figure 3. Equation of state for fcc, bcc and sc Ca. The three plus signs are experimental data from Anderson *et al* [21].

Table 4. Partial list of transition pressures for Ca and Sr. The abbreviations for the structures are: fcc = face-centred cubic; bcc = body-centred cubic; sc = simple cubic. The transition pressures are given in kbar.

Exp./Theo. + Ref.	fcc ⟶ bcc	bcc ⟶ sc
Ca		
Exp. Olijnyk + Holzapfel [6]	195	320
Theo. this work[a]	90–56	404–412
Theo. Ahuja *et al* [12]	150	330
Theo. Sofronkov *et al* [38]	59.6	
Theo. Sliwko *et al*[b] [11]	90 (?)	
Sr		
Exp. Olijnyk + Holzapfel [6]	35	
Exp. Jayaraman *et al*[c] [39]	35–18	
Exp. McWhan + Jayaraman[d] [19]	(15.7) 34.7	
Theo. this work[a]	19.5–22	
Theo. Animalu [7]	10	
Theo. Sofronkov *et al* [38]	37.7	
Theo. Mutlu[e] [40]	21–34	
Theo. Skriver [9]	40	

[a] In each column the first number does not, the second number does include the zero-point energy calculated in the Debye approximation.
[b] The authors write that the transition occurs at a reduced volume $V/V_0 \cong 0.58$, which corresponds to about 200 kbar, but their figure 6 shows that at that pressure the bcc phase has already a much lower energy than the fcc phase, whereas energy equality occurs at $V/V_0 \cong 0.82$, which corresponds to about 90 kbar.
[c] The first (second) number is the transition pressure measured upon increasing (decreasing) pressure.
[d] The authors give the transition pressure only in terms of 'applied load' (15.7), which we tentatively calculate from other reported data to correspond to 34.7 kbar.
[e] The two numbers were found with two different exchange–correlation potentials.

parameters of the fcc, bcc and sc phases as functions of pressure up to 500 kbar, and figure 3 shows the equation of state (the plus signs from the experiments of Anderson *et al* [14]).

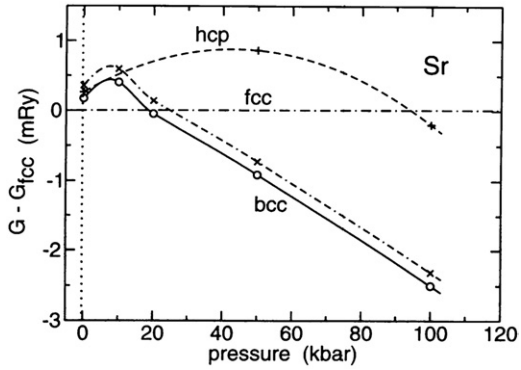

Figure 4. Free-energy differences for Sr bcc–fcc (circles and crosses) and hcp–fcc (plus signs) versus pressure. The circles exclude, the crosses include, zero-point energies.

4. Strontium

4.1. Review

Like Ca, Sr has an fcc ground state (Sr I) at $p = 0$; for Sr, as for Ca, the dominant experimental result in the low-pressure range remains that of Olijnyk and Holzapfel [6], who originally reported several pressure-induced transitions as follows: from fcc (Sr I) to bcc (Sr II) at 35 kbar; from bcc to an unidentified but probably orthorhombic phase (Sr III) at 260 kbar; then to an unknown phase (Sr IV) at 350 kbar; and finally to a complex phase (Sr V) similar to that of Ba IV at 460 kbar. The higher-pressure phases were later revised, first by Winzenick and Holzapfel [15], who claimed Sr III to be orthorhombic, and finally by McMahon *et al* [16] who found it to be tetragonal with the β-tin structure. The uppermost phase Sr V was shown by McMahon *et al* [16] to have the same incommensurate structure composed of a 'host' and two 'guest' components as Ba IV. The final sequence as it is known to date is given in table 1, second panel.

The theoretical studies concentrated on the zero-pressure ground state and on the fcc-to-bcc transition pressure. All except one [11] found both the correct (fcc) ground state and reasonable agreement with the experimental transition pressure at 35 kbar. More details are given in the next section.

4.2. Results and discussion

Our calculations focused on the fcc, the bcc and the hcp phases. At zero pressure the fcc phase is found to have lower energy than the bcc and hcp phases by about 0.17 and 0.27 mRyd/atom, respectively, and is therefore the ground state. The corresponding lattice parameters are listed together with others in table 2, second panel: our results agree with experiment within about 0.5% (two measured values differ by 0.2%). One previous calculation [12] also differs by 0.5%. Other calculated values [17, 18] differ by much more (about 5%). With increasing pressure the Gibbs free energies (at 0 K) of fcc and bcc cross at about 19.5 kbar, and the bcc phase becomes the ground state above that pressure (figure 4). All lattice parameters decrease with increasing pressure, of course, as depicted in figure 5, but comparison with experiment at $p > 0$ is limited to one pressure, the only one that we could find in the literature: McWahn and Jayaraman [19] reported the lattice parameter of bcc Sr at 42 kbar to be $a_{\mathrm{bcc}} = 4.434$ Å while the interpolation in our curve of figure 5 yields 4.378 Å, i.e., within 1.2%.

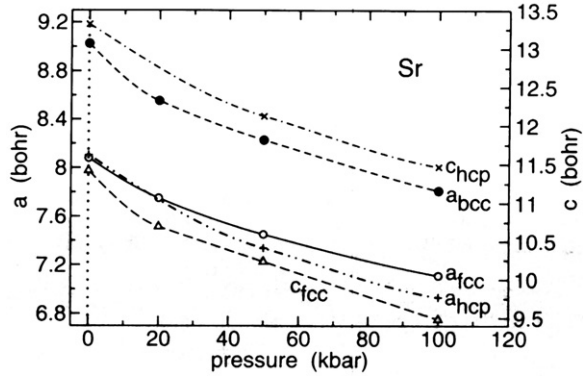

Figure 5. Pressure dependence of the lattice parameters of fcc, bcc and hcp Sr.

Estimates of the zero-point energies require, as mentioned above, knowledge of the elastic constants. The available experimental and theoretical data for fcc and bcc Sr are summarized in table 3, second panel. Just as for fcc Ca, there is a surprising discrepancy between reported experimental data, so a clear assessment of how well our results agree with experiment is not possible. We note again that some authors find both fcc and bcc Sr unstable ($C' < 0$). Our calculated fcc elastic constants at $p = 0$ listed in table 3 agree with one set of measured data [20] fairly well: c_{11} is 7% low, c_{12} 3% low, c_{44} 4% high. Other calculated values [17, 18] disagree much more. Our calculated bcc elastic constants listed in table 3 agree with measured values [21] (made at 930 K) as follows: c_{11} 28% high, c_{12} 27% high, c_{44} 110% high. However, elastic constants will be lower at higher temperatures. Other calculated values are further away [17, 18].

With our calculated elastic constants we find zero-point energies (in the Debye approximation) of 0.75 and 0.94 mRyd/atom for fcc and bcc Sr, respectively, at zero pressure (compared to 1.08 and 1.05 mRyd/atom from Animalu [7] and 1.07 and 1.01 mRyd/atom from Moriarty [8], respectively). Adding these contributions to the minimum free energies we find that the free-energy difference between fcc and bcc is increased. Assuming again, as for Ca, that this difference persists even at finite pressures, we see in figure 4 that the fcc-to-bcc transition is moved up to 23 kbar, improving the agreement with the experimental result of 35 kbar of Olijnyk and Holzapfel [6] (especially remembering the 'overestimate of the hydrostatic pressure component by 10 to 40 kbar'). Evaluating the elastic constants at $p = 10$ kbar and assuming linear dependence of the ZPE on p we find that the ZPE of bcc Sr increases by less than 1%, but the ZPE of fcc Sr increases by 25%. Hence the transition pressure for fcc to bcc Sr is increased by the ZPE just to 22 kbar rather than 23 kbar when the pressure dependence is ignored. Comparisons between experimental and theoretical transition pressures for Sr are summarized for convenience in table 4.

The equations of state for fcc, bcc and hcp Sr are depicted in figure 6. Here again we could find only limited experimental data [14], which are included in the figure as crosses.

5. Barium

5.1. Review

Experimental data for Ba are more recent and more complete than for Ca and Sr, thanks to the careful and well-executed study of Takemura in 1994 [22]. At zero pressure the ground state of

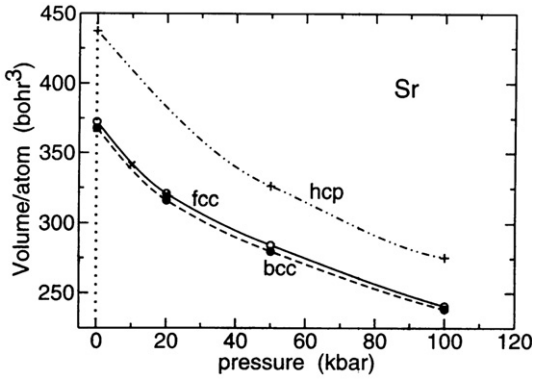

Figure 6. Equation of state for fcc, bcc and hcp Sr. The three crosses are experimental data from Anderson *et al* [21].

Ba (Ba I) is bcc rather than fcc, which has been explained as due to Ba having greater d-band occupation at $p = 0$ than Ca and Sr [23, 24]. Increasing p increases d-band occupation in Ca and Sr and brings about the transition from fcc to bcc, while increasing p in Ba changes the structure to hcp (Ba II) at 55 kbar. Beyond that pressure there was initially some confusion: in the 1960s and 1970s some anomalies in the electrical resistance and volume were interpreted as indicative of a transition at about 80 kbar to a new phase (Ba III) (see the references cited in [22]), but Takemura's study found no evidence for the existence of this phase III, and Ba III was therefore dropped from consideration in subsequent treatments of the subject. But a further well-defined transition occurs at 126 kbar to a new initially unidentified phase Ba IV. The structure of this phase was elucidated in 1999 by Nelmes *et al* [25] using single-crystal and powder diffraction x-ray data, and called 'self-hosting incommensurate': it is composed of a tetragonal 'host' with 'guest' chains along the c axis of the host. The chains form two different structures, one well crystallized and the other highly disordered, thus producing strong diffuse scattering, both chains being incommensurate with the host (see Heine's comment in *Nature* [26]). With further increasing pressure Ba undergoes yet another transition at 450 kbar to a phase (Ba V) with hcp structure. Thus, Ba has two hcp phases at finite pressures: one (Ba II) between 55 and 126 kbar and another (Ba V) above 450 kbar. The interesting features of these two phases are (1) that the axial ratio c/a of phase II decreases dramatically with increasing pressure from 1.575 to 1.498 and (2) that the c/a ratio of phase V remains almost pressure independent at a value of 1.575 up to 900 kbar, the maximum pressure reached in Takemura's experiment. Of great value in the corresponding paper are numerical data about the pressure dependence of the lattice parameters and volumes of phase I (bcc) and of phases II and V (both hcp). An overview of the whole sequence of Ba structures is given in table 1, third panel.

5.2. Results and discussion

Table 2, third panel, lists the available experimental data together with our results and some theoretical literature reports about the lattice parameters of bcc Ba at zero pressure and hcp Ba at 60 kbar. We find agreement with experiment within 0.7% for the bcc structure and within 0.5 and 1.2% for the a and c parameters, respectively, of the hcp structure.

The relative behaviour of the free energy of hcp Ba as compared to that of bcc Ba is summarized in figure 7 as the difference between the two. At zero pressure the ground state is

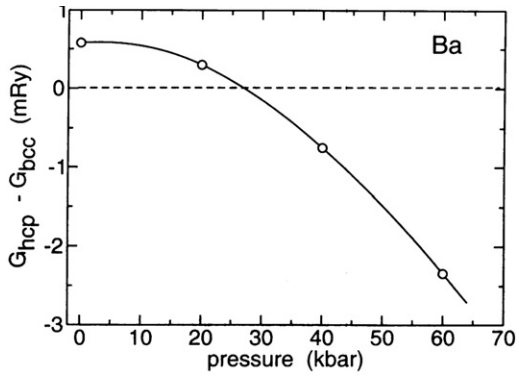

Figure 7. Difference between the Gibbs free energy (at 0 K) of hcp Ba II and that of bcc Ba I.

bcc, in agreement with experiment, and the G curves cross one another at about 28 kbar, only about $1/2$ of the experimental value at 55 kbar. Two possible reasons for this disagreement may be the following. (1) Chen *et al* [23] (who find the transition pressure at 11 kbar) state that experimentally the transition pressure decreases with decreasing temperature, but do not specify the rate. Hence we can only expect qualitatively that the discrepancy between our result (at 0 K) and experiment (at room temperature) would be reduced. (2) Our result does not include corrections for the ZPE of the two phases involved. We have calculated the elastic constants needed for this correction: for bcc Ba at zero pressure they are listed in table 3, third panel, where we find good agreement with the available experimental data within the stated experimental errors. For hcp Ba, also at zero pressure, we find the following values (not listed in table 3 because they involve six entries), in Mbar: $c_{11} = 0.020$, $c_{12} = 0.206$, $c_{13} = 0.038$, $c_{33} = 0.260$, $c_{44}^{\text{unrelaxed}} = 0.042$, $c_{33}^{\text{relaxed}} = 0.037$ (for the difference between unrelaxed and relaxed shear constants see [13]). These numbers show that $c_{11} < c_{12}$, and hence hcp Ba is unstable at zero pressure (for stability conditions see [27]); hence a ZPE correction at $p = 0$ is not possible. Qualitatively, we note that the presence of optical modes in hcp Ba (not present in bcc Ba) contributing to the ZPE would be expected to raise G for hcp Ba with respect to bcc Ba and push the transition to hcp to higher pressures.

However, the agreement between our calculated values and measured lattice parameters in all phases at all pressures is very satisfactory. Figure 8 depicts the calculated (circles) pressure dependence of the a parameter for both bcc and hcp Ba together with the experimental results (crosses) of Takemura [22]: for Ba I, between 0 and about 60 kbar, the agreement falls between 0.2 and 0.3%; for Ba II, between 60 and 120 kbar, within less than 1.3%; and for Ba V, between 450 and 900 kbar, within 0.6%. Figure 9, upper panel, shows the c parameter for Ba II, with theory and experiment essentially overlapping one another, and for Ba V, with agreement within 1.2%. The lower panel depicts the c/a ratio for both phases, agreement within 1.1% for Ba II and less than 2% for Ba V. This figure also confirms the result of Reed and Ackland [28] that phase II and phase V are indeed the same phase, contradicting an earlier statement [22] that the two are different crystallographic phases. The variation in c/a is due to a continuous transfer of electrons from s to d as p increases. This explanation was given earlier by Zeng *et al* [24], who dissected the band-structure wavefunctions to show the amounts of occupation of s, p, d and f orbitals as pressure increases in hcp Ba II and hcp Ba V. They showed that in Ba II between $p = 55$ and 126 kbar, where c/a drops abruptly, the occupation number of 5d orbitals goes from 1.2 to 1.4 per atom, while the occupation number of 6s orbitals goes from 0.55 to 0.37. However, in Ba V from

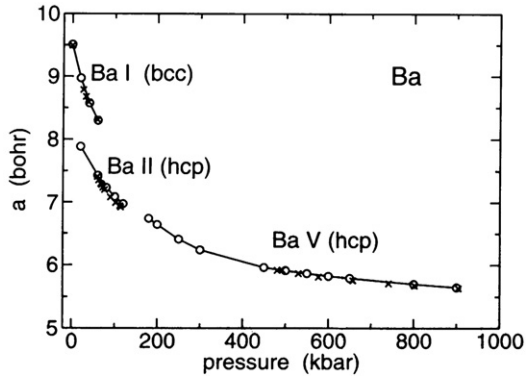

Figure 8. Calculated (circles on solid curve) and experimental (crosses) a parameter of bcc Ba I, hcp Ba II and hcp Ba V as functions of pressure.

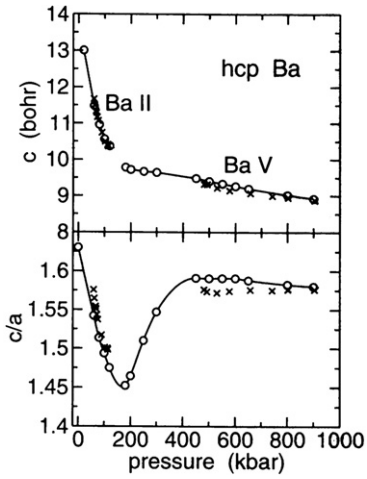

Figure 9. Calculated (circles on solid curve) and experimental (crosses) c parameter (upper panel) and axial ratio c/a (lower panel) of hcp Ba II and Ba V as functions of pressure.

$p = 480$ to 950 kbar, where c/a is nearly constant, the 6d and 5s occupation numbers are also constant.

Figure 4 of the paper by Reed and Ackland [28] provides a test of their procedure for calculating $(c/a)(p)$ versus ours. They did not use the usual procedure of $E(c/a)$ at constant V to find equilibrium structures, but minimized the enthalpy in a molecular dynamic calculation in the presence of an applied stress, and hence avoided use of the equation of state. Such molecular dynamic calculations have been criticized as using classical equations of motion at $T = 0$ K where quantum mechanics is required [29]. We note that the $(c/a)(p)$ curves in figure 4 of [28] deviate from the measurements of Takemura [22] considerably more than in our figure 9, i.e., the calculated c/a values of Ba II in [28] decrease less rapidly with increasing pressure than experimental values, and the calculated c/a values in Ba V keep rising as p increases, whereas the measured values are nearly flat.

Finally, figure 10 shows the equation of state for Ba I, II and V, with good agreement between theory and experiment.

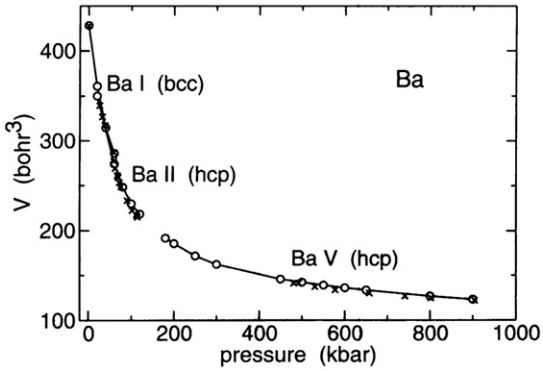

Figure 10. Calculated (circles on solid curve) and experimental (crosses) equation of state for bcc and hcp Ba.

6. Discussion

We have applied the MNP [4] and the EBP [5, 13] procedures to a computational study of Ca, Sr and Ba under pressure based on minimizing G. For all three elements we find good agreement with experimental data on the lattice parameters at zero pressure. We have condensed concisely in one table the experimental results of structural studies at finite pressures, and have calculated the Gibbs free energies (at 0 K) of all three elements as functions of lattice parameters and pressure. Experimental data for the lattice parameters at finite pressures are scarce for Ca and Sr, much better for Ba: for all three we display full pressure dependences, in good agreement with whatever experimental data are available, mostly better than other theoretical results published in the literature.

Our calculated transition pressures (pressures at which the Gibbs free energies of the two competing phases equal one another) are not in good agreement with experimental results. The discrepancies are explainable only partly with declared experimental uncertainties (for Ca and Sr) and partly with temperature effects. We have introduced a correction of the transition pressures due to the zero-point energies, for which we have developed a procedure based on the Debye approximation. This procedure requires knowledge of the elastic constants of both phases involved in a transition. We have therefore calculated the elastic constants for Ca, Sr and Ba at zero pressure. Agreement with experimental data is good where such data are clearly reliable, otherwise uncertain where (as is the case for Ca and Sr) the experimental data from different sources disagree with one another. On the basis of the calculated elastic constants the zero-point-energy correction is found to increase the discrepancy with experiment for Ca, but to decrease it for Sr. For Ba, where the hcp phase turns out to be unstable at zero pressure, we presented qualitative arguments that would reduce the discrepancy with experiment.

Especially significant, we think, is the excellent agreement with the careful and extensive pressure data of Takemura on Ba [22], which cover a large pressure range in three phases. The agreement provides good support for the accuracy of lattice parameters at about the 1% level for the data, the WIEN band-structure programs and our procedure.

We believe that the greater accuracy of our procedure compared with the usual procedure of minimizing the energy E as a function of c/a at constant volume V is due, among other factors, to:

(1) the need in the procedure based on E to find an accurate equation of state $E(V)$ and differentiate it to fix the pressure p;

(2) the fact that E has a *constrained* minimum at equilibrium as a function of a and c, i.e., has a minimum only for constant volume at finite pressure, whereas G has a true minimum for all variations of a and c around equilibrium.

These difficulties with the calculation of equilibrium based on minimizing E are computational difficulties, and can be overcome by careful calculation. However, the molecular dynamics calculation of Reed and Ackland [28], which is carried out at constant applied stress, also avoids the use of the equation of state $E(V)$, and also minimizes G to find the equilibrium structure. As mentioned above, this procedure has been criticized [29] for using classical equations of motion at 0 K, where quantum equations are needed. This difficulty may be an inherent difficulty of the molecular dynamics procedure and indeed our calculated curves for $(c/a)(p)$ for Ba II and V in figure 9 are much closer to the experimental data than the curves in figure 4 of [28].

Appendix. Calculation of the zero-point energy of cubic crystals in the generalized Debye approximation

The Debye approximation expresses the zero-point energy (ZPE) of a vibrating Bravais crystal lattice in terms of a single parameter Θ_D [41, page 53]:

$$\mathrm{ZPE} = \tfrac{9}{8} k_B \Theta_D, \tag{A.1}$$

$$\Theta_D = \frac{\hbar \bar{v}}{k_B} \left(\frac{6\pi^2}{V_0} \right)^{1/3}, \tag{A.2}$$

where $\hbar$ is the Planck constant (over 2π), k_B the Boltzmann constant, V_0 the volume per atom and $\bar{v}$ an average elastic wave velocity. The original form of the Debye approximation assumed an isotropic solid so that the three velocity branches were isotropic. The generalization of the Debye approximation used here is to make the velocities of the long wavelength (acoustic) waves functions of direction in the crystal. This directional dependence is obtained from the elastic equations of motion (see, e.g., [41], page 139). Then

$$\bar{v} = \left(\frac{12\pi}{I} \right)^{1/3} \tag{A.3}$$

$$I = \int_{4\pi} \mathrm{d}\Omega \sum_{j=1}^{3} \frac{1}{v_j^3} \equiv \int_{4\pi} \mathrm{d}\Omega \, f(\theta, \phi). \tag{A.4}$$

The eigenvalues of the 3×3 propagation matrix, elements Γ_{ij}, are $\rho v_j^2(\hat{n})$ where ρ is the crystal density

$$\rho = \frac{m}{V_0}, \tag{A.5}$$

m is the atomic mass and $\hat{n}$ is a unit vector in the direction of propagation, orthogonal components n_1, n_2, n_3.

For cubic lattices

$$\begin{aligned} \Gamma_{ii} &= c_{11} n_i^2 + c_{44}(1 - n_i^2), \qquad i = 1 \text{ to } 3, \\ \Gamma_{ij} &= (c_{12} + c_{44}) n_i n_j, \qquad i \neq j, \quad i, j = 1 \text{ to } 3. \end{aligned} \tag{A.6}$$

The c_{ij} are the elastic constants in Voigt notation ([41], p.37).

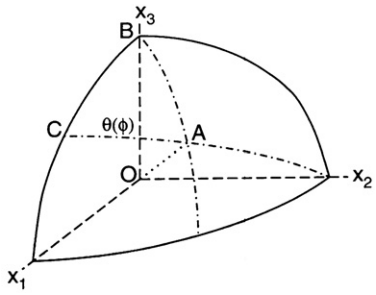

Figure A.1. Octant of a sphere. The spherical triangle ABC is 1/48th of the sphere and the integration region of (A.7).

Table A.1. Six-point Gaussian integration parameters for spherical triangle ABC in figure A.1.

x_i	are the Gaussian argument values between 0 and 1 0.033 765 2429, 0.169 395 3068, 0.380 690 4070 0.619 309 5930, 0.830 604 6932, 0.966 234 7571
w_i	are the Gaussian weight factors for six-point integration 0.085 662 2462, 0.180 380 7865, 0.233 956 9673 0.233 956 9673, 0.180 380 7865, 0.085 662 2462
θ_i	are θ values on the CA boundary of spherical triangle of integration ABC at Gaussian values of ϕ 0.785 573 97, 0.789 836 29, 0.808 080 82 0.846 880 84, 0.899 322 30, 0.943 089 80

Equation (A.6) applies also to finite hydrostatic pressure, where the c_{ij} are the coefficients relating stresses and strains added to the finite pressure and compression, respectively [42].

The wave velocities in any direction in the crystal are quickly evaluated by modern eigenvalue programs. The only remaining substantial computational problem is the integral I, for which many procedures have been developed (for a review see Alers [43]). An efficient accurate procedure was used here which exploits cubic symmetry and Gaussian integration formulae over 1/48 th of the 4π solid angle for all directions. Thus

$$I = 48 \int_0^{\pi/4} \mathrm{d}\phi \int_0^{\theta(\phi)} \sin\theta \, \mathrm{d}\theta f(\theta, \phi), \tag{A.7}$$

where the integration is over the directions in the spherical triangle ABC in figure A.1. Then I can be accurately approximated by a sum of 36 terms using one six-point Gaussian formula for the θ- and one for the ϕ-integration, on the basis of the integration formula [44]

$$\int_0^1 f(x)\,\mathrm{d}x \cong \sum_{i=1}^{6} w_i f(x_i). \tag{A.8}$$

Hence

$$I = 48\frac{\pi}{4} \sum_{i=1}^{6} w_i \theta_i \sum_{j=1}^{6} w_j \sin(\theta_{ij}) f(\theta_{ij}, \phi_i), \tag{A.9}$$

where

$$\phi_i = \frac{\pi x_i}{4}, \qquad i = 1 \text{ to } 6, \tag{A.10}$$

and on the side AC of the spherical triangle ABC in figure A.1

$$\theta_i = \theta(\phi_i), \qquad i = 1 \text{ to } 6, \tag{A.11}$$

and

$$\theta_{ij} = x_j \theta_i, \qquad i, j = 1 \text{ to } 6. \tag{A.12}$$

The values of x_i, w_i, θ_i are given in table A.1 so the calculation of Θ_D can be readily duplicated. The 36 terms of (A.9) with the entries in table A.1 integrate $\sin\theta$ over ABC to eight-figure accuracy.

References

[1] Blaha P, Schwarz K, Masden G K H, Kvasnicka D and Luitz J 2001 *WIEN2k, An Augmented Plane Wave + Local Orbitals Program for Calculating Crystal Properties* (Kalheinz Schwarz, Techn. Universität Wien, Austria) (ISBN 3-9501031-1-2)

[2] Hohenberg P and Kohn W 1964 *Phys. Rev.* B **136** 864
Kohn W and Sham L J 1965 *Phys. Rev.* B **140** A1133

[3] Cottenier S 2002 *Density Functional Theory and the Family of (L)APW-Methods: a Step-by-Step Introduction* Instituut voor Kern-en Stralingsfysica, KU Leuven, Belgium, ISBN 90-807215-1-4 (to be found at http://www.wien2k.at/reg_user/textbooks)

[4] Marcus P M and Jona F 2005 *Eur. Phys. J.* B **45** 39

[5] Marcus P M, Jona F and Qiu S L 2002 *Phys. Rev.* B **66** 064111

[6] Olijnyk H and Holzapfel W B 1984 *Phys. Lett.* A **100** 191

[7] Animalu A O E 1967 *Phys. Rev.* **161** 445

[8] Moriarty J A 1973 *Phys. Rev.* B **8** 1338
Moriarty J A 1986 *Phys. Rev.* B **34** 6738

[9] Skriver H L 1982 *Phys. Rev. Lett.* **49** 1768

[10] Wentzcovitch R M and Krakauer H 1990 *Phys. Rev.* B **42** 4563

[11] Sliwko V L, Mohn P, Schwarz K and Blaha P 1996 *J. Phys.: Condens. Matter* **8** 799

[12] Ahuja R, Eriksson O, Wills J M and Johansson B 1995 *Phys. Rev. Lett.* **75** 3473

[13] Jona F and Marcus P M 2001 *Phys. Rev.* B **63** 094113
Jona F and Marcus P M 2002 *Phys. Rev.* B **66** 094104
Jona F and Marcus P M 2003 *J. Phys.: Condens. Matter* **15** 7727

[14] Anderson M S, Swenson C A and Peterson D T 1990 *Phys. Rev.* B **41** 3329

[15] Winzenick M and Holzapfel W B 1996 *Phys. Rev.* B **53** 2151

[16] McMahon M I, Bovornratanaraks T, Allan D R, Belmonte S A and Nelmes R J 2000 *Phys. Rev.* B **61** 3135

[17] Mehl M J and Papaconstantopoulos D 1996 *Phys. Rev.* B **54** 4519

[18] Pollack L, Perdew J P, He J, Marques M, Nogueira F and Fiolhais C 1997 *Phys. Rev.* B **55** 15544

[19] McWhan D B and Jayaraman A 1963 *Appl. Phys. Lett.* **3** 129

[20] Brandes E A and Brook G B (ed) 1992 *Smithells Metals Reference Book* 7th edn (Oxford: Butterworth–Heinemann)

[21] Mizuki J and Stassis C 1985 *Phys. Rev.* B **32** 8372
Mizuki J and Stassis C 1987 *Phys. Rev.* B **35** 872 (erratum)

[22] Kenichi T 1994 *Phys. Rev.* B **50** 16238

[23] Chen Y, Ho K M and Harmon B N 1988 *Phys. Rev.* B **37** 283

[24] Zeng W-S, Heine V and Jepsen O 1997 *J. Phys.: Condens. Matter* **9** 3489

[25] Nelmes R J, Allan D R, McMahon M I and Belmonte S A 1999 *Phys. Rev. Lett.* **83** 4081

[26] Heine V 2000 *Nature* **40** 836

[27] Nye J F 1964 *Physical Properties of Crystals* (Oxford: Clarendon)

[28] Reed S K and Ackland G J 2000 *Phys. Rev. Lett.* **84** 5580

[29] Quong A A and Liu A Y 1997 *Phys. Rev.* B **56** 7767

[30] Donohue J 1974 *The Structure of the Elements* (New York: Wiley)

[31] Pearson W B 1967 *A Handbook of Lattice Spacings and Structures of Metals and Alloys* vol 2 (Oxford: Pergamon)

[32] Chen Y, Ho K-M, Harmon B N and Stassis C 1986 *Phys. Rev.* B **33** 3684

[33] Stassis C, Zaretsky J, Misemer D K, Skriver H L, Harmon B N and Nicklow R M 1983 *Phys. Rev.* B **27** 3303

[34] Heiroth M, Buchenau U, Schober H R and Evers J 1986 *Phys. Rev.* B **34** 6681

[35] Wang G M, Papaconstantopoulos D A and Blaisten-Barojas E 2003 *J. Phys. Chem. Solids* **64** 185

[36] Buchenau U, Heiroth M, Schober H R, Evers J and Oehlinger G 1984 *Phys. Rev.* B **30** 3502

[37] Öztekin Çiftci Y and Çolakoğlu K 2001 *Turk. J. Phys.* **25** 363

[38] Sofronkov A N, Drozdov V A and Pozhivatenko V V 1992 *The Physics of Metals and Metallography* vol 74, p 140 (Engl. Transl.)
[39] Jayaraman A, Klement W Jr and Kennedy G C 1963 *Phys. Rev.* **132** 1620
[40] Mutlu R H 1996 *Phys. Rev.* B **54** 16321
[41] Wallace D C 1972 *Thermodynamics of Crystals* (New York: Wiley)
[42] Barron T H K and Klein M L 1965 *Proc. Phys. Soc.* **85** 52
[43] Alers G A 1965 *Physical Acoustics* vol III, ed W P Mason (New York: Academic) pp 1–42
[44] Abramowitz M and Stegun I A (ed) 1964 *Handbook of Mathematical Functions* (*Applied Mathematics Series*) vol 55 (Washington, DC: National Bureau of Standards) p 921